Physical Chemistry: An Indian Journal
ISSN: 0974-7524
**Research Article** | Vol 18 Iss 1

# Computational Study of an Antimalarial Quinone Methide Pentacyclic Triterpenoid Derivative Isolated from *Salacia leptoclada* Tul (Celastraceae)

**Issofa Patouossa[1,2*], Gloria Kabuo Sifa[3], Jason Thambwe Kilembe[2,3], Bienfait Kabuyaya Isamura[2,3,4,] Koto-te-Nyiwa Ngbolua[5], Virima Mudogo[3], Jules Tshishimbi Muya[2,3]**

[1]Department of Analytical Chemistry, University of Yaounde, Yaounde, Cameroon

[2]Department of Theoretical Chemistry and Physics, University of Kinshasa, Kinshasa, DR Congo

[3]Department of Chemistry, University of Kinshasa, Kinshasa, DR Congo

[4]Department of Chemistry, Rhodes University, Makhanda, South Africa

[5]Department of Biology, University of Kinshasa, Kinshasa, Democratic Republic of the Congo

[*]**Corresponding author:** Issofa Patouossa, Department of Analytical Chemistry, University of Yaound, Yaounde, Cameroon, Tel: 693181788; E-mail: patouossa12@yahoo.fr

**Received:** October 16, 2022, Manuscript No. TSPC-22-77417; **Editor assigned:** October 18, 2022, PreQC No. TSPC-22-77417 (PQ); **Reviewed:** November 01, 2022, QC No. TSPC-22-77417; **Revised:** January 10, 2022, Manuscript No. TSPC-22-77417 (R); **Published:** January 17, 2022, DOI: 10.37532/0974-7524.23.18.166

## Abstract

**DFT calculations and polarizable continuum model are employed to elucidate the structure and reactivity of a naturally occurring quinone methide pentacyclic triterpenoid derivative isolated from *Salacia Leptoclada* Tul (Celastraceae). Our computational results reveal that the lowest stereoisomer is more stabilized in less polar solvents. The interaction energies between the stereoisomer with water and adenine at B97D3/6-31++G(d,p) amount to -9 kcal/mol and -17 kcal/mol. Furthermore, theoretical spectra of the lowest stereoisomer are first reported for experimental characterization. Molecular docking calculations indicate that the molecule binds in the groove of double-helical DNAs to guanosine and adenosine bases owing to hydrogen interaction.**

***Keywords: Quinone methide pentacyclic triterpenoid; Density Functional Theory (DFT); Time Dependent DFT (TDDFT); Polarizable Continuum Model (PCM); Molecular Electrostatic Potential (MEP); Molecular docking***

## Introduction

Over the past few decades, the world has been confronted to a series of devastating outbreaks, the most recent being the ongoing COVID-19 pandemic whose first case was declared in Wuhan, China in December 2019 [1,2]. There is no doubt; all of these public health problems have caused significant damages in terms of human loss and economic crisis. Still, malaria has remained the biggest nightmare for the populations in sub-Saharan Africa, causing about 3 million deaths and almost 5 billion clinical cases every year [3]. Sadly, the majority of its victims are children under the age of five years. Malaria is transmitted exclusively through the bites of anopheles mosquitoes. The intensity of transmission depends on a series of factors related to the parasite, the vector, the human host and the environment [4,5]. In contrast with the abundant knowledge amassed on this disease and the alarming data reported by the world health organization, facts are that humanity is still far away from winning over this calamity. This hypothesis can be supported by the fact that more and more validated antimalarial drugs are ejected from the market due to their progressive loss of activity as induced by the resistance of some types of plasmodium [6,7]. As such, there is a pressing need to identify and validate new effective drugs against malaria [8-10].

One of the most documented approaches in the drug discovery pipeline of antimalarial drugs involves isolating pure compounds from plants and testing their biological activity against various species of *plasmodium* [11]. In this rationale, Ngbolua and his coworkers isolated a quinone methide pentacyclic triterpenoid derivative from *Salacia leptoclada*Tul

**Citation:** Patouossa I, Sifac GK, Kilembe JT, et al. Computational Study of an Antimalarial Quinone Methide Pentacyclic Triterpenoid Derivative Isolated from *Salacia leptoclada* Tul (Celastraceae). Phys Chem Ind J. 2023;18(1):166

(Celastraceae), which they showed to exhibit (*in vitro*) antiplasmodial activity against the chloroquine resistant strain FC29 of *Plasmodium falciparum* with an $IC_{50}$ value of (0.052 ± 0.030) µg/ml and cytotoxic effect on murine P388 leukemia cells with $IC_{50}$ value of (0.041 ± 0.020) µg/mL [12,13].

Nevertheless, since their work, no further study has been reported in the aim to figure out the reason behind these properties. We do believe that the starting point for such a long term goal can reside in a detailed understanding of the geometry and reactivity of this molecule. The present study is a contribution to elucidating the origin of the bioactivity and cytotoxicity of our compound of interest by providing fundamental insights into its structure and reactivity.

It is worth noting that investigations reported in this study rely on the demonstrated assumption that the biological properties of drugs strongly depend on their structure and the interactions they develop with other compounds in biological environment. Noteworthy is that by inspecting figure, one should notice the presence of several rotatable bonds, which suggest the existence of various stereoisomers. Unfortunately, no information has yet been reported discussing structural preferences and relative stability of these stereoisomers. In this study, we attempt to address this question using the density functional theory. More precisely, our focus is turned onto the geometric structure, molecular properties and reactivity of the lowest lying stereoisomer of the compound reported here and displayed in figures, both in the gas phase and in different solvents such as water, acetonitrile and chloroform. Finally, due to the reported cytotoxicity of the isolated molecule, investigations by molecular docking between isomeric molecules and DNA were done for analyzing the biologic behavior of our isomeric molecules.

## Materials and Methods

### Computational details

The pentacyclic triterpenoid derivative studied has five methyl groups attached to 1 (Figure 1a), which are geometrically oriented out of the molecular plane, shown in red color (Figure 1b). These methyl groups can be arranged above or below the molecular plane, in thirty two different configurations, giving rise to different stereoisomers. Detailed information on the binary code used for the identification of the 32 stereoisomers is provided in the supplementary information. These stereoisomers were optimized and vibrational modes computed at B3LYP and B97D3 [14,15]. To assess the influence of the basis sets on the relative stability of stereoisomers, STO-3G, 6-31G(d) and 6-$31^{++}$G(d,p) basis sets were also employed. Conformational analysis of the global minimum was carried out to identify the preferred torsion angle of the ester carbonyl group. The effect of solvents (e.g: Water, acetonitrile and chloroform) on the stability of the ground state electronic structure of the most stable stereoisomer was investigated in the framework of the Polarizable Continuum Model (PCM) [16]. Furthermore, the hydrogen bonding interaction between the stereoisomer and some basic molecules, *viz*: Water and adenine, were investigated at the B97D3/6-$31^{++}$G(d,p) level. Frontier molecular orbitals (HOMO and LUMO) and Molecular Electrostatic Potential (MEP) were used as DFT reactivity descriptors also computed were the theoretical spectra, *viz.* Infrared (IR), Ultraviolet-Visible (UV-VIS), Vibrational Circular Dichroism (VCD) and Nuclear Magnetic Resonance (NMR) of this molecule. All calculations above were carried out utilizing Gaussian 09 package [17-21]. For visualization purposes, Gaussview 4.1 and Chemcraft programs were used.

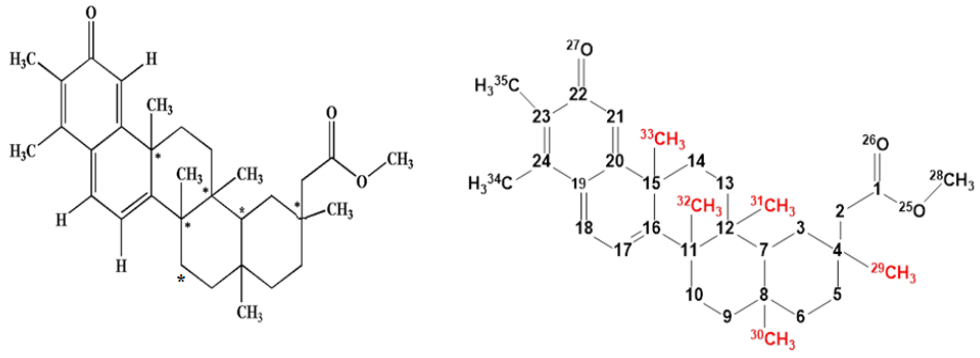


FIG. 1. **a). Schematic representation of the isolated compound by Ngbolua and co-workers. b). The out of plane methyl groups are represented using red color and the H atoms are omitted for clarity.**

Molecular blind docking calculations were performed using MGL tools 1.5.7 with AutoGrid4 to determine grid box, protein and ligand preparation, finally auto dock vina for setting up docking calculation between isolated ligand and DNA sequence using Linux interface. CT-DNA sequence d(CGCGAATTCGCG)2 dodecamer (PDB ID: 1BNA) were retrieved from the protein data bank receptor (DNA). The receptor was enclosed in a box with the following number of grid points in x=62, y=68, z=122 and a grid centre set to x=15.589 Å, y=20.947 Å, z=10.596 Å, with a grid spacing of 0.375 Å. DNA dodecamer was kept rigid during docking. Discovery studio 2020 client software was used for modelling non-bonded polar and hydrophobic contacts in DNA binding site.

## Results and Discussion

### Gas-phase geometries and energetics

Stereoisomers characterized by the same orientation of the H atom attached to C7 (Asymmetric carbon not bound to $CH_3$) with respect to the ester group are referred to in the present study as cis-stereoisomers. Table 1 lists relative energies, HOMO-LUMO gaps and dipole moments of the sixteen cis-stereoisomers optimized at B3LYP and B97D3 levels employing 6-$31^{++}$G(d,p) basis sets.

Figure 2 illustrates the geometry of the most stable cis-stereoisomer and the trends of relative energies of all cis-stereoisomers computed at the B3LYP level of theory with different basis sets. The trend of the relative energies suggests that 1 and 16 are thermodynamically the most and least stable among cis-isomers, respectively. Their energy difference is estimated to be ~23 kcal.mol$^{-1}$ at both B3LYP and B97D3 with 6-$31^{++}$G(d,p). This indicates that the methyl groups prefer to be oriented as described in 1. The lowest energy isomer 1 is 2 kcal.mol$^{-1}$ calculated at B97D3/6-$31^{++}$G(d,p) below 2. This lowest structure is characterized by the highest HOMO-LUMO gap energy of 1.89 eV calculated at B97D3/6-$31^{++}$G(d,p) level (3.14 eV at B3LYP/6-$31^{++}$G(d,p). This finding suggests that 1 is also the most kinetically stable or least reactive within cis-stereoisomers. Also noteworthy is that B3LYP tends to overestimate the HOMO-LUMO gap as compared to B97D3. However, the two methods yield similar trends in the calculated dipole moment values. A comparison between the performance of basis sets is illustrated in Figure 2b reveals that relative energies calculated at B3LYP/6-31G(d) are in agreement with those evaluated using 6-$31^{++}$G(d,p) basis set. Therefore, 6-31G(d) basis in conjunction with the B3LYP functional offers a good compromise between cost and accuracy for the study of these particular molecular systems. With this in mind, we were more confident to optimize trans-isomers at the B3LYP/6-31G(d) level.

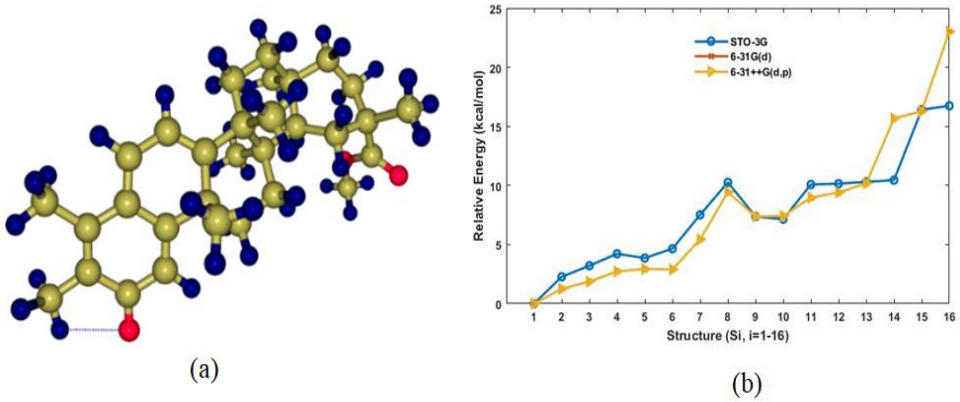


FIG. 2. **a). Optimized geometry of the most stable cis-isomer (S1) and; b). influences of basis sets on the relative energies of cis-stereoisomers at B3LYP level.**

The relative energies of our isomers depend on the orientation of the methyl groups. For instance, when the methyl groups are spatially close to each other, the total energy of the molecular system increases due to the columbic repulsion. The steric effect arising from the interaction between adjacent methyl groups is expected to influence the C-C bond lengths of the molecular framework. Figure 3a illustrates the C-C bond lengths of different six-membered rings of the lowest and highest structures. Geometrical differences between these two isomers should provide further information about their thermodynamic stability. Note that the lowest energy structure exhibits shorter bond lengths than the highest energy one. A diagram showing the change in selected C-C bonds of all optimized stereoisomers is given in the electronic supplementary information.

To establish the optimum orientation of the ester carbonyl group, a one dimensional potential energy surface scan was performed by varying the $C_{28}$-$O_{25}$-$C_1$-$C_2$ dihedral angle at B3LYP/STO-3G* level. The resulting potential energy profile is illustrated in Figure 3b. The potential energy surface scan was performed in 24 steps and the dihedral angle was varied from 23.5° to 383.5°, with an increment of 15°. As shown in Figure 3b, the global minimum is located at the dihedral angle of 233.5°. Additionally, two local minima are also located and are energetically situated 0.5 and 0.8 kcal.mol$^{-1}$ above the lowest energy conformer. These structures are characterized by a $C_{28}$-$O_{25}$-$C_1$-$C_2$ dihedral angle of 8.5 and 113.5 degrees, respectively.

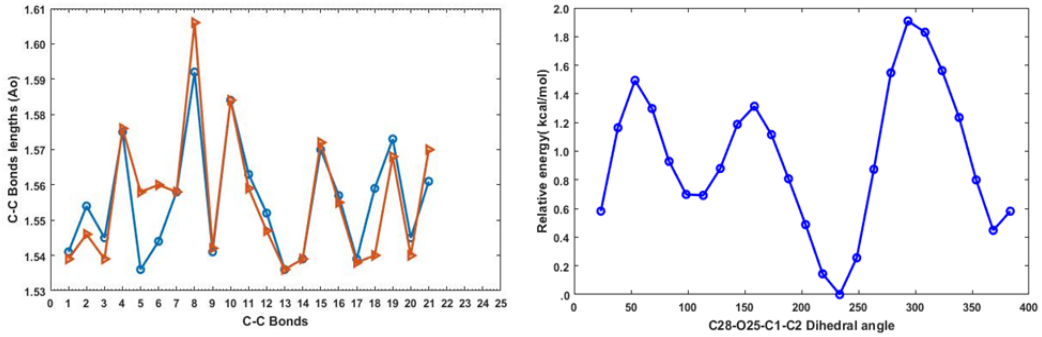


(a) (b)

FIG. 3. **a). C-C bonds lengths for the most stable (1) and least stable stereoisomer (16); b). The one dimensional potential energy surface scan for the rotation around C1-O25 bond.**

The relative energies (RE in kcal/mol), the HOMO-LUMO gaps (H-L in eV) and the dipole moments (μ in D) of all the stereoisomers computed at B97D3/6-31$^{++}$G(d,p) level and value obtained at B3LYP/6-31$^{++}$G(d,p) in parenthesis are given in Table 1 below. These results suggest that optimized geometries are more stable when C7-H is in trans orientation with respect to the ester group, while its neighboring $CH_3$ fixed on the cycle prefers up/down alternations. 1 trans-isomer is 5.58 kcal.mol$^{-1}$ more stable than its corresponding cis-isomer at B3LYP/6-31G(d), while 7 trans-isomer is found to be nearly 3 kcal.mol$^{-1}$ more stable than 1.

TABLE 1. **Relative Energies (RE), HOMO-LUMO gaps (H-L) and dipole moments (μ) of all the stereoisomers computed at B97D3/6-31$^{++}$G(d,p) level. The data obtained at B3LYP/6-31$^{++}$G(d,p) are given in parenthesis.**

| Stereoisomers | RE/kcal.mol$^{-1}$ | H-L/eV | μ/D |
|---|---|---|---|
| 1[a] | 0.00 (0.00) | 1.89 (3.14) | 7.89 (6.53) |
| 2 | 2.04 (1.26) | 1.83 (3.08) | 6.81 (6.59) |
| 3 | 2.38 (1.81) | 1.83 (3.10) | 6.11 (6.18) |
| 4 | 2.72 (3.06) | 1.81 (3.09) | 5.18 (5.70) |
| 5 | 3. 56 (3.20) | 1.81 (3.11) | 5.80 (4.53) |
| 6 | 3. 75 (3.78) | 1.86 (3.03) | 7.23 (7.24) |
| 7 | 6.72 (5.52) | 1.82 (3.16) | 8.03 (7.96) |
| 8 | 8.41 (9.61) | 1.72 (3.16) | 6.12 (5.31) |
| 9 | 8.66 (7.53) | 1.88 (3.09) | 7.16 (6.89) |
| 10 | 9.12 (7.42) | 1.88 (3.10) | 7. 61 (7.59) |
| 11 | 9.73 (8.94) | 1.87 (3.09) | 4.50 (3.97) |
| 12 | 9.85 (9.00) | 1.88 (3.09) | 4.55 (3.93) |
| 13 | 10.4 (9.86) | 1.80 (3.15) | 7.39 (7.36) |

| | | | |
|---|---|---|---|
| 14 | 16.1 (15.4) | 1.83 (3.17) | 5.30 (5.17) |
| 15 | 17.0 (16.2) | 1.87 (3.20) | 5.51 (5.50) |
| 16 | 23.5 (23.0) | 1.83 (3.17) | 6.56 (6.53) |
| a. The total electronic energy values of the most stable structure represented by the code {00101} have been evaluated to be -1431.46685 H (B97D3 level) and 1432.3403497 H (B3LYP level). | | | |

**Effect of solvent and chemical reactivity**

After identifying the most stable structure (trans 1) in the gas phase, additional calculations were performed to understand the effect of the solvent (water, chloroform and acetonitrile) on its stability by applying the polarizable continuum model of solvation. These solvents were chosen in such a way to cover a wide range of polarity. The relative energies of the most stable isomer optimized at B3LYP/6-31G(d) level in different solvents environments are listed in Table 2. This table suggests that this stereoisomer is stabilized in weakly polar solvents. Note that the relative energies in chloroform and acetonitrile media are quite similar. In addition, the solubility of this isomer appears to be influenced by the dipole moment and the permittivity of solvents.

TABLE 2. **Relative Energies (RE), HOMO-LUMO gap (H-L), dipole moment (ε) and relative dielectric constant (ε) of the low lying structure in different solvents considered in the present study.**

| **Medium** | **RE/kcal.mol$^{-1}$** | **H-L/eV** | **μ/D** | **ε** |
|---|---|---|---|---|
| Vacuum | 0.00 | 3.22 | 5.95 | 1.00 |
| Chloroform | -18.9 | 3.18 | 9.94 | 4.71 |
| Acetonitrile | -18.9 | 3.17 | 11.0 | 35.6 |
| Water | -10.2 | 3.15 | 13.1 | 78.3 |

The Highest Occupied Molecular Orbital (HOMO) and the Lowest Unoccupied Molecular Orbital (LUMO) in the most stable stereoisomer are shown in Figure 4, displays the Molecular Electrostatic Potential (MEP). The frontier molecular orbitals are of π character and have large contributions from the aromatic hydrocarbon units. Since the reactivity of the molecule depends on the frontier molecular orbitals, this region of the molecule is suspected to be important in its reactivity. A close inspection of the MEP reveals that the oxygen atom directly attached to the benzene ring is the most electron rich center in the molecule. As such, this oxygen atom is predicted to be the most preferred site for electrophilic attack.

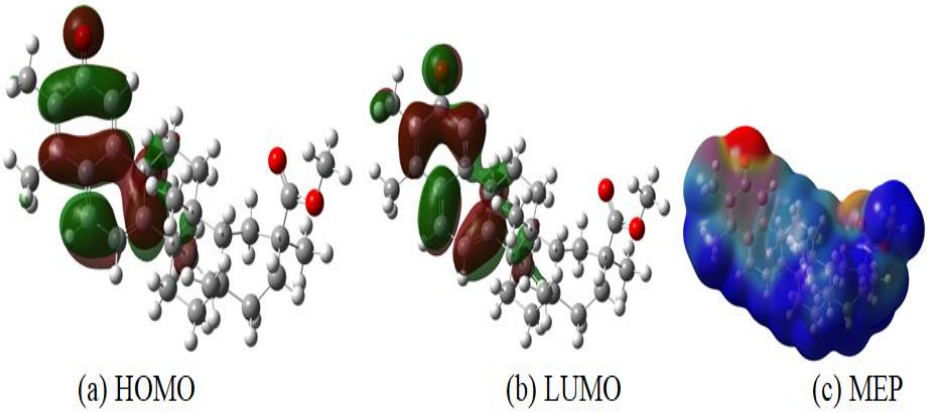


FIG. 4. **a,b). Frontier molecular orbitals and; (c) Molecular Electrostatic Potential (MEP).**

To probe the local reactivity of this stereoisomer, water and adenine (which can establish hydrogen bonds) were bound to

oxygen atoms. Figure 5 shows groove binding in the region of rich G-A bases pairs with a certain preference site of the binding in the cytosine base. The values of the interaction energies displayed in figure show that water forms a more stable complex when it interacts with the carbonyl of the benzene ring.

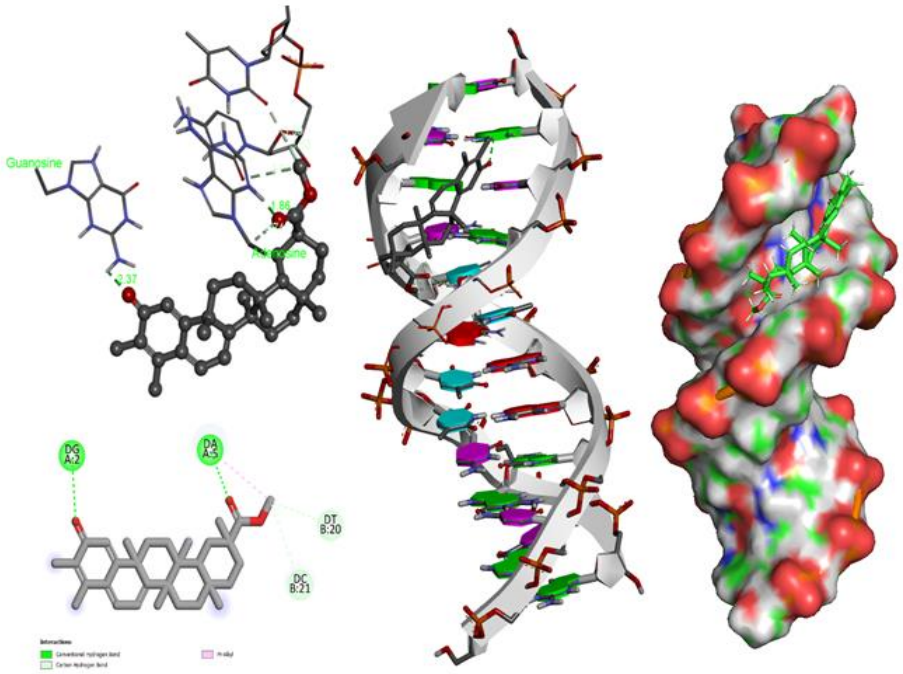


FIG. 5. **a-d). Groove binding in the region of rich G-A bases pairs with a certain preference site of the binding in the cytosine base.**

The optimized complexes obtained at B97D3/6-31$^{++}$G(d,p) are depicted in Figures 6 and 7. To evaluate the strength of the hydrogen bond in complex, interaction energy was computed as the energy difference between complex and reactants (isomer and basic molecule). The interaction energy corrected from the Basis Sets Superposition Errors (BSSE) is about -9.48 kcal.mol$^{-1}$ at B97D3/6-31$^{++}$G(d,p) level. In the case of adenine, the interaction with the carbonyl group gives rise to six different complexes. The calculated interaction energy corrected from BSSE at B97D3/6-31$^{++}$G(d,p) is largest when adenine is in orientation b. Further, the interaction energy (accounting for BSSE) between adenine and thymine computed at the same theory level is -20.70 kcal.mol$^{-1}$ and is almost approaching the hydrogen bonding energy of -17.27 kcal.mol$^{-1}$ for the complex formed between adenine and the stereoisomer of figures. The second lowest energy complex with adenine displays a stacked geometry of adenine characterized by stacking interaction energy of -15.64 kcal.mol$^{-1}$.

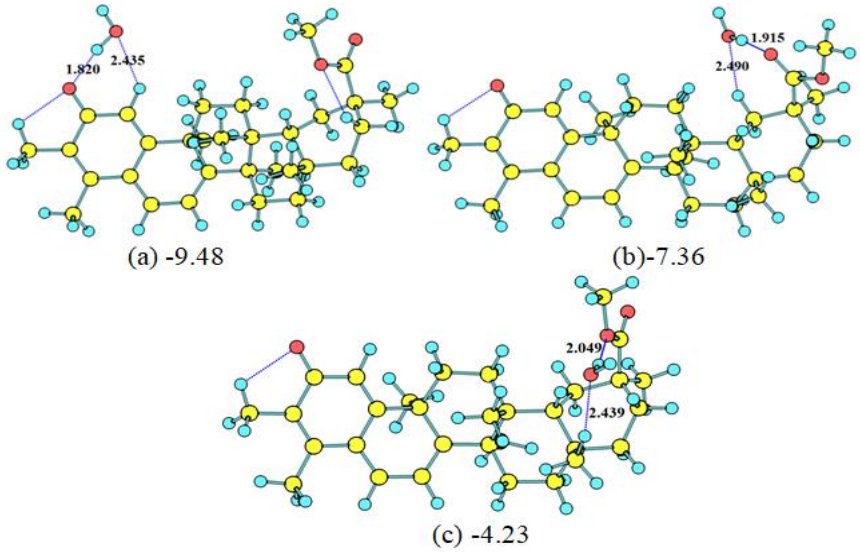


FIG. 6. **Optimized hydrogen bonds geometries and binding energies corrected from BSSE in kcal.mol$^{-1}$ of the complexes with water at B97D3/6-31$^{++}$G(d,p).**

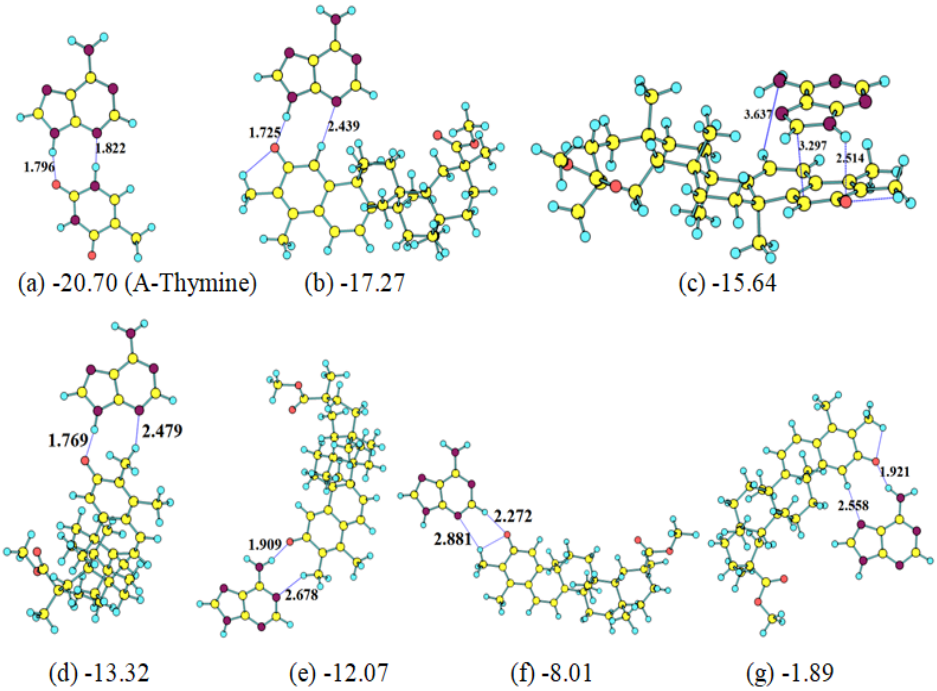


FIG. 7. **Optimized hydrogen bonds geometries and binding energies corrected from BSSE in kcal.mol$^{-1}$ of the complexes with adenine at B97D3/6-31$^{++}$G(d,p).**

**Molecular docking on DNA**

Molecular docking technique plays a significant role in drug design and elucidation of mechanisms of action of drugs. It is here used to get insight into the interaction between the isolated molecule and DNA. The binding affinities obtained from docking DNA with the isomeric molecules of isolated compounds are given in Table 3.

TABLE 3. **Molecular docking results of Binding Affinity (BA) with DNA.**

| Receptor | Stereoisomers | BA/kcal.mol$^{-1}$ |
|---|---|---|
| **DNA (PDB ID: 1BNA)** | 1 | -9.0 |
| | 10 | -9.0 |
| | 11 | -8.4 |
| | 12 | -8.0 |
| | 13 | -9.0 |
| | 14 | -8.5 |
| | 15 | -8.6 |
| | 16 | -8.9 |
| | 2 | -8.9 |
| | 3 | -8.2 |
| | 4 | -9.5 |
| | 5 | -9.1 |
| | 6 | -9.1 |
| | 7 | -8.1 |
| | 8 | -8.7 |
| | 9 | -8.8 |
| | 5-ASA[a] | -4.1 |
| | CMB[b] | -5. 9 |

This table reveals that the binding affinity range from -9.4 kcal.mol$^{-1}$ to -8.2 kcal.mol$^{-1}$. Compared to a small molecule docked in the same region by Shahabadi, et al., and Charak and coworkers which were ranged between -4.216 kcal mol$^{-1}$ and -5.91 kcal mol$^{-1}$ respectively, all isomers tested with DNA have higher binding affinities. Molecular docking results for the set of 17 isomers showed that almost all isomers are bound in the groove of double helical DNA and all optimal docking results were in the DG-DA rich region. Thus, high ranking isomeric molecules bound relatively easily to the minor groove of double stranded DNA, with some preference for adenosine and guanosine bases. From the optimal energy docking results, it comes out that the isomeric molecule 4 is trapped into the minor groove of the DNA fragments and is engaged into two hydrogen bonds with guanosine and adenosine as given in Table 4 below.

TABLE 4**. Hydrogen bonds derived from docking of DNA with isomer 4.**

| Atoms | DNA nucleotide bases | Distance/Å | Angle/$^{o}$ |
|---|---|---|---|
| $O^{26}$ | HN-Adenosine | 1.86 | 155 |
| $O^{27}$ | HN-Guanosine | 2.37 | 141 |

The complex formed is mainly stabilized by typical hydrogen bonds between the ketonic oxygen atom of isomer 4 and the Guanosine NH residues of the DNA fragment. This interaction is long of 2.37 Å. A second hydrogen bond involving the carbonyl group and Adenosine NH has a bond length of 1.86 Å. Nevertheless, other interactions like unconventional hydrogen bond (CH carbonyl group with the DNA bases in the Adenosine region, the Adenosine-ligand H-bond), π stacking interaction and hydrophobic interactions contribute to the stability of the complexes. This result indicates that Guanosine and Adenosine bases have a preference to interact with DNA fragments to some extent. Docking studies reveal that our molecule interacts with DNA through Adenosine and Guanosine located in the region supported by the MEP calculation result. The cis isomeric 4 shows a strong interaction with DNA estimated at -9.5 kcal.mol$^{-1}$. The latter is 0.4 kcal.mol$^{-1}$ stronger than cis-isomeric 1.

**Spectroscopic properties**

To support the experimental characterization of the present stereoisomer, theoretical spectra (IR, UV visible and VCD) of the most stable stereoisomer were carried out and depicted in Figure 8. The harmonic vibrational frequencies were calculated at B3LYP/6-31G(d) level. The IR spectrum of the most stable stereoisomer is depicted in figures. Some characteristic modes can be noticed, especially the symmetric stretching of the ester carbonyl group appearing at 1767 $cm^{-1}$ and the vibrations of the benzene rings in the region between 1700 $cm^{-1}$ and 1575 $cm^{-1}$. The ultraviolet visible spectrum was computed at the TD-B3LYP/ 6-31G(d,p) level and is represented in Figures. This spectrum shows an intense peak at 388.80 nm and is assigned to the electronic transition between HOMO and LUMO. The vibrational circular dichroism spectrum computed at the same level of theory is represented in Figures. The absolute configuration of the most stable structure belongs to RRSSR. It is to be noted that no experimental data on the spatial position of atoms of the present stereoisomer has been reported so far. Due to this reason, assigning peaks should be considered with caution.

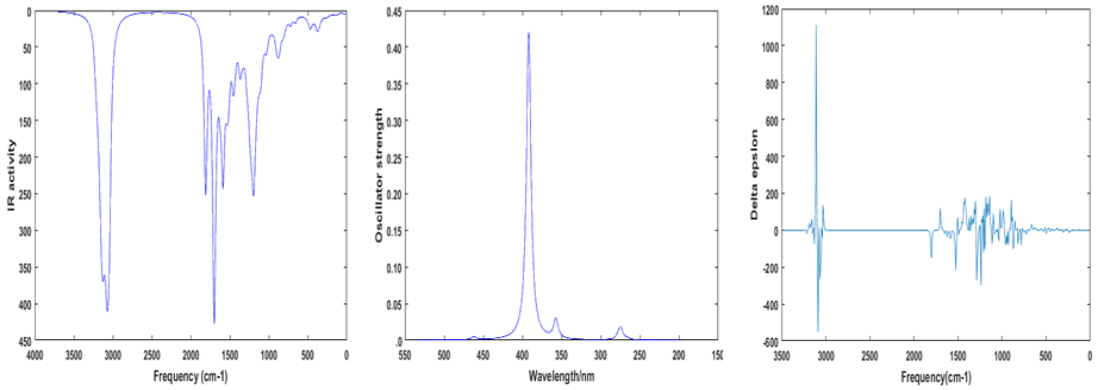


FIG. 8**. Spectra of the most stable cis-stereoisomer in vacuum: (a) IR; (b) UV-VIS; (c) VCD at B3LYP/6-31G; (d) level.**

## Conclusion

B3LYP and B97D3 are employed to investigate the lowest stereoisomer of naturally occurring quinone methide pentacyclic triterpenoid derivative, from *Salacia Leptoclada* Tul (Celastracea*e*). Our computational results reveal that the lowest stereoisomer is more stabilized in less polar solvents such as chloroform and acetonitrile. The interaction energy corrected from basis set superposition errors between the stereoisomer with water is about -9 $kcal.mol^{-1}$ while that of adenine is estimated at -17 $kcal.mol^{-1}$ at B97D3/6-$31^{++}$G(d,p). Further, theoretical spectra were also elucidated to support its experimental characterization. Molecular docking studies indicate that all isomers form stable complexes with the DNA in the groove of double helical DNAs and draw its stability from a series of interactions, especially hydrogen bonds to guanosine and adenosine bases.

## Conflict of interest

The authors declare that they have no conflict of interest.

## Acknowledgement

The authors thank Dr. Carol Parish for a fruitful cooperation and access to University of Richmond supercomputer.

## References

1. Jacob ST, Crozier I, Fischer WA, et al. Ebola virus disease. Nat Rev Dis Prim. 2020;6(1):13.
2. Ciotti M, Ciccozzi M, Terrinoni A, et al. The COVID-19 pandemic. Crit Rev Clin Lab Sci. 2020;57(6):365-388.
3. Rowe AK, Rowe SY, Snow RW, et al. The burden of malaria mortality among African children in the year 2000. Int J Epidemiol. 2006;35(3):691-704.

4. Lindsay SW, Birley MH. Climate change and malaria transmission. Ann Trop Med Parasitol. 1996;90(5):573-588.
5. Paloque L, Ramadani AP, Mercereau-Puijalon O, et al. *Plasmodium falciparum*: Multifaceted resistance to artemisinins. Malar J. 2016;15:149.
6. Tuteja R. Malaria-An overview. FEBS J. 2007;274(18):4670-4679.
7. Wiesner J, Ortmann R, Jomaa H, et al. New antimalarial drugs. Angew Chem Int Ed Engl. 2003;42(43):5274-5293.
8. Schlitzer M. Antimalarial drugs-What is in use and what is in the pipeline. Arch Pharm (Weinheim). 2008;341(3):149-163.
9. Pillay P, Maharaj VJ, Smith PJ. Investigating South African plants as a source of new antimalarial drugs. J Ethnopharmacol. 2008;119(3):438-454.
10. Ruphin FP, Baholy R, Emmanue A, et al. Antiplasmodial, cytotoxic activities and characterization of a new naturally occurring quinone methide pentacyclic triterpenoid derivative isolated from *Salacia leptoclada* Tul. (Celastraceae) originated from Madagascar. Asian Pac J Trop Biomed. 2013;3(10):780-784.
11. Persch E, Dumele O, Diederich F. Molecular recognition in chemical and biological systems. Angew Chem Int Ed Engl. 2015;54(11):3290-3327.
12. Becke AD. Density functional exchange energy approximation with correct asymptotic behavior. Phys Rev A Gen Phys. 1988;38(6):3098-3100.
13. Grimme S, Antony J, Ehrlich S, et al. A consistent and accurate ab initio parametrization of Density Functional Dispersion correction (DFT-D) for the 94 elements H-Pu. J Chem Phys. 2010;132(15):154104.
14. Ramirez R, Borgis D. Density functional theory of solvation and its relation to implicit solvent models. J Phys Chem B. 2005;109(14):6754-6763.
15. Fukui K, Yonezawa T, Shingu H. A molecular orbital theory of reactivity in aromatic hydrocarbons. J Chem Phys. 1952;20(4):722-725.
16. Politzer P, Murray JS. Quantitative analyses of molecular surface electrostatic potentials in relation to hydrogen bonding and co-Crystallization. Cryst Growth Des. 2015;15(8):3767-3774.
17. Dadkhah S, Bagheri Novir S. Computational investigation of structural and electronic properties of cis and trans structures of fluvoxamine as a nano drug. Comput Theor Chem. 2017;1105:33-45.
18. Kasende OE, Matondo A, Muzomwe M, et al. Interaction between temozolomide and water: Preferred binding sites. Comput Theor Chem. 2014;1034:26-31.
19. Kasende OE, Muya JT, Broeckaert L, et al. Theoretical study of the regioselectivity of the interaction of 3-methyl-4-pyrimidone and 1-methyl-2-pyrimidone with Lewis acids. J Phys Chem A. 2012;116(33):8608-8614.
20. Trott O, Olson AJ. AutoDock Vina: Improving the speed and accuracy of docking with a new scoring function, efficient optimization and multithreading. J Comput Chem. 2010;31(2):455-461.
21. Charak S, Shandilya M, Tyagi G, et al. Spectroscopic and molecular docking studies on chlorambucil interaction with DNA. Int J Biol Macromol. 2012;51(4):406-411.